The 2012 World Congress on
Advances in Civil, Environmental, and Materials Research (ACEM' 12)
Seoul, Korea, August 26-30, 2012

Aerodynamic Performance Comparison of Head Shapes for High-Speed Train at 500KPH

*Kai Cui[1)], Xiuping Wang [2)], Shouchao Hu [2)], Taiyuan Gao [2)]

[1), 2)] *State Key Laboratory of High Temperature Gas Dynamics, Institute of Mechanics, Chinese Academy of Science, Beijing, 100190*
[1)] kcui@imech.ac.cn

ABSTRACT

The aerodynamic performance of simplified configuration of trains with three carriages at a speed of 500km/h, in which the head and tail shapes are randomly selected from two typical shapes of **ROCKET**(short for **R**) and **SWORD**(short for **S**), is analyzed by numerical simulation method. The results indicate that aerodynamic performance is influenced by the shapes of head and tail within high speed train. Symmetrical configuration with **R** head and **R** tail has the largest aerodynamic drag, while symmetrical configuration with S head and S tail has the least aerodynamic drag. However, unsymmetrical configuration with **S** head and **R** tail is both of less aerodynamic drag for three carriages and of less absolute value of lift for the tail carriage. Compared with symmetrical configurations, unsymmetrical configuration performs better both in drag and lift. Besides, by changing the length of streamlined part of train head within above configurations, the influence of aerodynamic drag by slenderness ratio has been studied. It shows that the slenderness ratio of head affects aerodynamic drag in some extent. As slenderness ratio of **S** is 8.3 and **R** 8.0, aerodynamic performance becomes the optimal. There should be an optimal slenderness ratio for other train head shapes. These conclusions can provide some valuable references for practical design of train shapes.

1. INTRODUCTION

According to the Davis equation, aerodynamic drag is proportional to the square of train speed. As a result, most of the train drag is caused by aerodynamics with the speed-up of high speed train. From some experimental results of real trains, aerodynamic drag of the traditional train at the speed of 120km/h occupies 40% of total drag, trains with blunt head at the speed of 160km/h, accounts for 75%, while train at the speed of 300km/h with a 10-meters long streamlined-head takes up for 75% (Tian 2007). The literature (Baker 2010) described the flow field around the train, especially the head and tail region. Aerodynamic performance is closely related to shapes of head

[1)] Associate Professor
[2)] Graduate Student

and tail and is necessary to optimize the head and tail shape of high speed train(Tian 2007, Raghunathan 2002, Wang 2011, Liang 2002). Developed countries like Japan, Germany have taken the optimization design of head shape in aerodynamic as a key technology, and there arises the special research field, i.e., high speed train aerodynamics.

Vytla (Vytla 2010) aimed at finding the optimum shape of a two dimensional nose shape of a high speed train at the speed of 350km/h considering both the induced aerodynamic drag and the generated aerodynamic noise. The results show that the optimization algorithm suggested requires a small number of simulations to identify the optimum shape compared with other methods. The nose shape should be slightly short and pointed to get the best aerodynamic performance in terms of induced drag and the nose shape should be slightly long and little blunt for the least aerodynamic noise generated. Lee (Lee 2008) dealt with design of three-dimensional nose shape of high-speed train to minimize the maximum micro-pressure wave, which is known to be mainly affected by train speed, train-to-tunnel area ratio, slenderness ratio, slenderness and shape of train nose, etc. Ku (Ku 2010) used the central constitution design method to choose the design data to build the response model. With the gradient type BFGS method to reduce the micro pressure wave when train entering a tunnel. Comparing to the original shape, the maximum micro pressure of the optimized shape has been reduced by 12%~19%. Krajnović (Krajnovićm 2009) has presented a new procedure for optimization of aerodynamic properties of trains. Instead of large number of evaluation of Navier-Stockes solver, simple polynomial response surface models are used as a basis for optimization. Besides, the essay (Anthoine 2007) and the essay (Kikuchi 2011) take the sonic boom and micro pressure as the optimization objectives, respectively, to optimize the head shape. And good results have been obtained. The above references clearly show that the head and the tail shape plays an important role in the design work of a high speed train.

With the rapid development of high speed train in China, Chinese researchers paid more and more attention to high speed train aerodynamics. Tian (Tian 2006) put forward that increasing the length of streamlined train head can effectively improve aerodynamic performance. The results of her research show that compared with other types of head shapes, pointed spindle shape is of relatively less aerodynamic drag and absolute value of the lift. Chen (Chen 1998) investigated the characteristic of drag by wind tunnel tests. The results revealed the influence of slenderness ratio of the head on aerodynamic drag when the wind speed has reached 50m/s. When the slenderness ratio of the train head increase from 1.716 to 3.654, the greater the slenderness ratio, the smaller the drag coefficient is and the tail of a train is more sensitive to the slenderness ratio. The study of Tian and Liang (Tian 2003) showed that the aerodynamic performance of double-arch head performs better than single-arch ones, while the regulation is the exact opposite for tails. Sun (Sun 2010) proposed an efficient optimization approach aiming at the optimizing the head shape of CRH3. Chen and Zeng (Chen 2009) simulated the aerodynamic performance of train with several shapes of train head. The numerical result shows if the head shape is contracted from the back to the nose, the train performs better in aerodynamics.

In summary, many researchers have already studied the relationship between the head shape and the aerodynamic performance, and it shows that the shape and the

slenderness ratio of the head have great impacts on the aerodynamic drag, lift and micro-pressure wave etc. However, their researches were limited to the train for which head and tail is of the same shape and speed is a little bit lower (limited within 300km/h). It is obviously that the aerodynamic performance will be more and more important as the train is speed-up. It remains unknown whether the symmetrical train configuration still performs best, whether the slenderness ratio of the streamlined part influence the aerodynamic performance in the same way as the train running at a higher speed.

The present status naturally motivates our study. In this paper, a numerical simulation work for evaluating the aerodynamic performance of unsymmetrical train configurations at the speed of 500km/h has been carried out. The head and tail shapes of train configurations with three carriages are selected from two typical train shape ROCKET (short for R) and SWORD(short for S). In four composed configurations, there are two symmetrical trains, R-R and S-S (the first letter stands for head shape and the second letter stands for the tail shape), and two unsymmetrical configurations, R-S and S-R. The flow fields around train configurations have been numerical simulated and analyzed in detail. The results indicate that the aerodynamic performance is influenced by shapes of head and tail. The symmetrical configuration with R head and R tail produces the largest aerodynamic drag, and symmetrical configuration with S head and S tail produces the least aerodynamic drag while unsymmetrical configuration with S head and R tail is of less aerodynamic drag and absolute value of lift for tail. Compared with symmetrical configurations, the unsymmetrical configuration performs better in both drag and lift. Besides, by changing the length of streamlined part of train head within above configurations, influence of aerodynamic drag by slenderness ratio has been also studied. It shows that slenderness ratio influences aerodynamic drag to a certain extent. As slenderness ratio of S is 8.3 and R 8.0, aerodynamic performance becomes the optimal. There should be an optimal slenderness ratio for other train head shapes.

2. TRAIN MODELS

The high-speed train is of relatively complicated. Fig. 1 depicts an entire train configuration with three-carriages. Because this paper aims at the aerodynamic influenced by the shape of head and tail, three-carriage train is simplified, such as ignoring the finite structure like the door handles, the inside and outside windshield and the pantograph. Fig. 2 demonstrates the simplified train configuration. In this way, we can not only focus on head and tail shape but also facilitate the creation of high-quality computation grids which improves the calculation accuracy and efficiency.

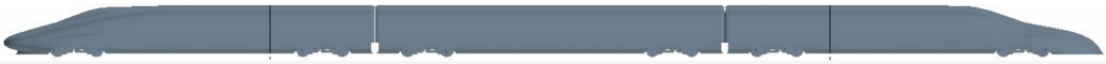

Fig. 1. Train configuration without simplification

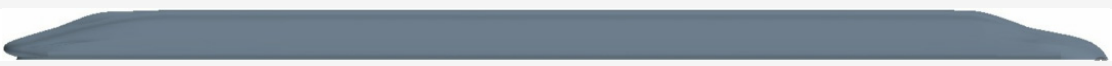

Fig. 2. Train configuration with simplification

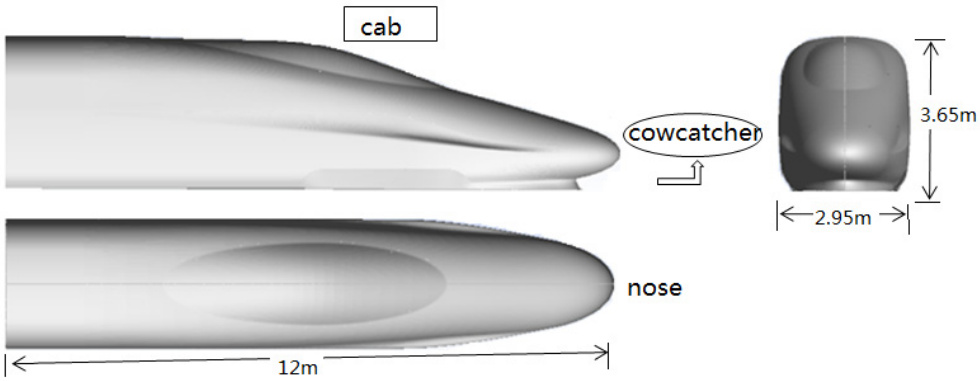

Fig. 3. The streamlined part of ROCKET (R)

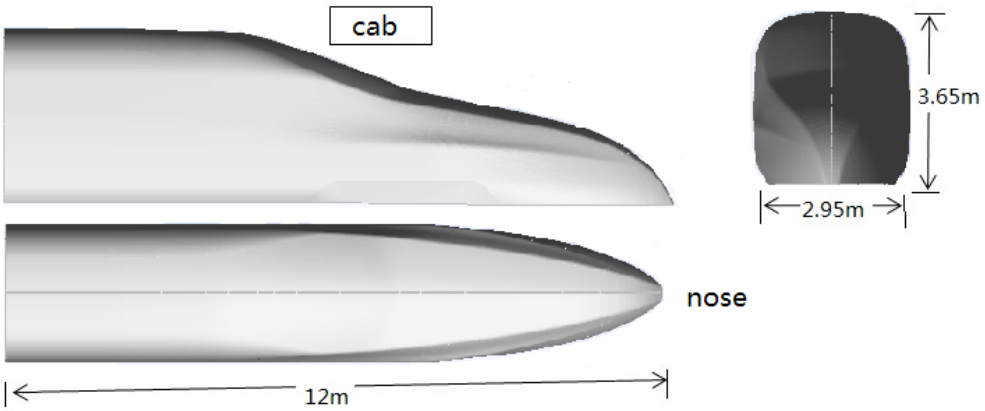

Fig. 4 The streamlined part of SWORD (S)

Fig. 3 and Fig. 4 demonstrated the head shape of R and S. The length of the stream part of both heads is 12m, the height of front window cab is 2.45m, the length of the middle car is 25.5m, the height is 3.65m, and the width is 2.95m.

3. NUMERICAL MODULE AND COMPUTATIONAL GRIDS

The widely-used commercial computational fluid dynamics software Fluent is used to simulate the flow field around the train. The 3D compressible RANS solver is adopted. The Roe scheme is used as the spatial discretization scheme. The computational conditions are as follows. The speed of the train is 500 kilometer per hour (KPH), i.e. the Mach number is 0.40706. The pressure of far field is 101325 (pa). .The ground is of moving wall condition with velocity of 138.8889 (m/s). The no-slip wall boundary condition is used in the surface of the train.

The computational field is given as follows to diminish the disturbance of the far field boundary in a subsonic flow field. A [-400m, 400m] field and a [-0.176m, 200m] field are given in X and Z direction respectively, while a [0m, 200m] field is given in Y direction because only half model is considered in this direction.

An unstructured textrahegron-prism hybrid grid structure is used to discretize the

whole computational area, illustrated as Fig. 5. Several layers of prismatic grids are arranged near the train wall to capture the boundary layer. The grids of the far field are tetrahedral grids.

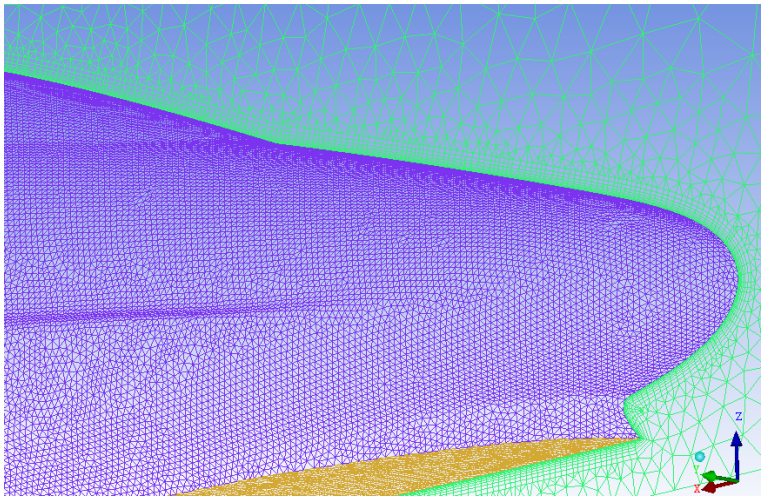

Fig. 5. Illustration of computational grids

In order to verify the reliability of the numerical results and minimize the error caused by the computation grids as much as possible, a grid convergence test is carried out at first. The process is as follows. Based on the R-R train configuration, three different meshes have been generated with the wall grid scale in 50mm and the far field grid scale 10000mm unchanged. The details are listed in the Table 1. The difference of three meshes is the thickness of the first grid, ranking from 3.5mm to 0.035mm. To make the transition of the grids from the boundary grids to the tetrahedral grids smoothly, the number of the boundary layers has been corresponding increased.

The maximum error of the total drag coefficients is about 1.7%. Therefore, the difference of results from three meshes can be neglected and the numerical results are reliable. As the mesh size affects the computation and convergence time to some extent, it is reasonable to choose the first kind of mesh to make the subsequent numerical simulation. Though the train configurations vary from each other, the total mesh quantity remains 700,000.

Table 1 Numerical results of the grid convergence tests

Case	Height of the first layer/mm	layer number	Grid quantity	cd
1	3.5	9	668	0.17173
2	0.35	17	1035	0.17240
3	0.035	25	1400	0.16946

4. AERODYNAMIC ANALYSIS OF FOUR CONFIGURATIONS

The aerodynamic drags of four train configurations are listed in Table 2. It can be

seen that R-R configuration has largest aerodynamic drag and S-S the smallest. The drags are different by 3.0%. Aerodynamic drags of R-R and R-S are similar, and so it is with S-R and S-S; drag of R-R and S-R are quite different, and so it is with R-S and S-S, which illustrates that it is head shape rather than tail shape has greater impact than tail on aerodynamic drag.

Table 2 Aerodynamic drag of the four configurations

Configurations	all	Head	Middle	Tail
R-R	0.17173	0.07388	0.04080	0.05705
R-S	0.16738	0.07292	0.03934	0.05512
S-R	0.16672	0.06850	0.03959	0.05863
S-S	0.16638	0.06913	0.04108	0.05617

Note: the first letter stands for the head shape, and the latter one stands for the tail shape.

For above four configurations, drag coefficients for head occupied 43%, middle 24%, and tail 33% of all drag, respectively. The aerodynamic drags of R are larger than that of S for both head and tail. Thus, S is preferable as the head and tail as to aerodynamic drag. The unsymmetrical train performs better partly because that the middle carriage has less aerodynamic drag.

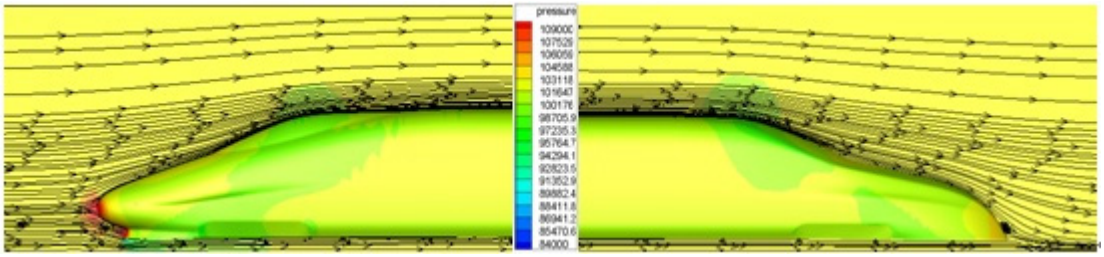

Fig. 6. Pressure contours for the three-carriage train R-S

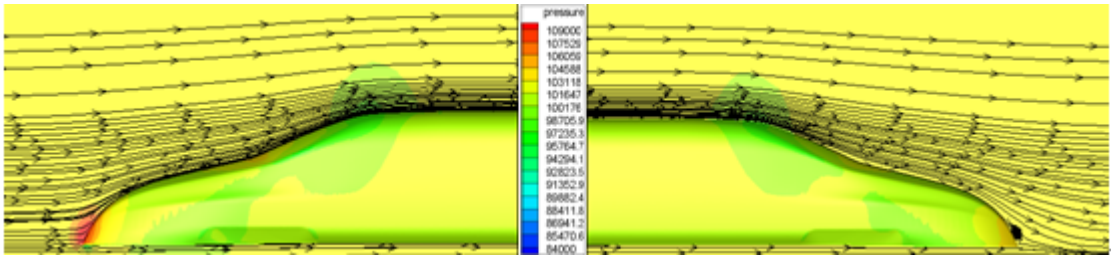

Fig. 7. Pressure contours for the three-carriage train S-S

Fig. 6 described the pressure contours around the R-S configuration. And the pressure contours mainly affected by the flow field around train wall. The flow speed from the far field gradually slows down and flows to top and lower surface when it approaches the nose sharp. On the nose tip, air speed is reduced to 0, where the high pressure area exists. The down-flowing air gradually speeds up and once again air speed slow down to 0 at the cowcatcher region, and then the air reaches the gap

between the cowcatcher and the sub grade where the air reaches the fastest speed due to the decrease of the flow area according to Bernoulli Principle. The air flowing to top of train surface speeds up along the surface and there exists another less high-pressure area for there is a slight angle between the train nose and the window. After that, the air flow speeds up again and becomes the fastest at the end of the window.

Pressure contours around S head is a little different from that of R head, shown in Fig. 7. Firstly, there is no cowcatcher and the nose is more near to the ground within S head. Secondly, the streamlined parts of the heads are quite different. Due to the nose of the S head is nearer to the ground than R, the amount of air flows to top surface is larger than air flows to lower surface. As a result, the low-pressure area at the front of lower surface is less weak with less high-pressure area at the window stronger.

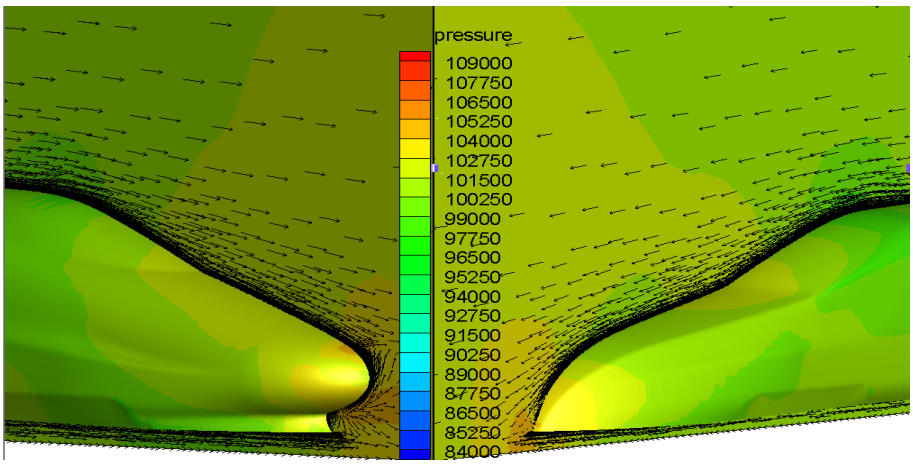

Fig. 8. Velocity vectors of the two tails

Fig. 8 demonstrates the pressure contours around the tail. It shows that flow around S is regular. There is flow separation around the R in tail, which contributes to the increase of aerodynamic drag.

From the above analysis, different train shapes generate different flow field and pressure contours on train. As a result, the aerodynamic drag varies from one configuration to another. For the wheel-rail train system, neither positive lift nor negative lift is good for train efficient operation. Therefore, the closer to zero the absolute value, the better train performs.

Table 3 Lift coefficient for the four train geometry model

Configuration	Head	Middle	Tail	all
R-R	-0.12639	0.00032	-0.01000	-0.13607
R-S	-0.12455	-0.00020	0.07566	-0.04908
S-R	-0.10668	-0.00053	-0.01306	-0.12027
S-S	-0.10921	0.00048	0.07508	-0.03365

Table 3 shows the lift distribution. Lift coefficients of heads are negative, and R is large than S in absolute value of lift. For Tails, R is less than S in absolute value in lift.

As tail lift is closely related to train stability, it is reasonable that R performs better than S.

The lift coefficients in the middle car depend on configuration of train. For symmetrical train, the lift is positive while in the unsymmetrical train, negative. As a result, the unsymmetrical train is more stable with the middle train.

Considering only the aerodynamic drag, the aerodynamic performance of the symmetrical train S-S is an optimal configuration. When considering the aerodynamic drag along with lift, S-R is preferable, for which absolute value of aerodynamic lift in tail and drag is less. In practical, it is necessary to design the head and tail shape separately, for it is more efficient to obtain the optimal train configurations with more optimal aerodynamic performances.

5 AERODYNAMIC DRAG CHANGES BY HEAD SLENDERNESS RATIO

Fig. 9 shows aerodynamic drag of head streamlined part. The aerodynamic drag can be classified into two types: friction drag and pressure drag. It is clear that R head and S head perform quiet differently in aerodynamic drag. The frictions are similar but the pressure drag are quiet different to each other. R head is more in pressure drag. This part is to study the relationship between slenderness ratio and aerodynamic drag. S-S and R-S configurations are taken into account. It is also feasible to compare above relationships between symmetrical and unsymmetrical train configurations.

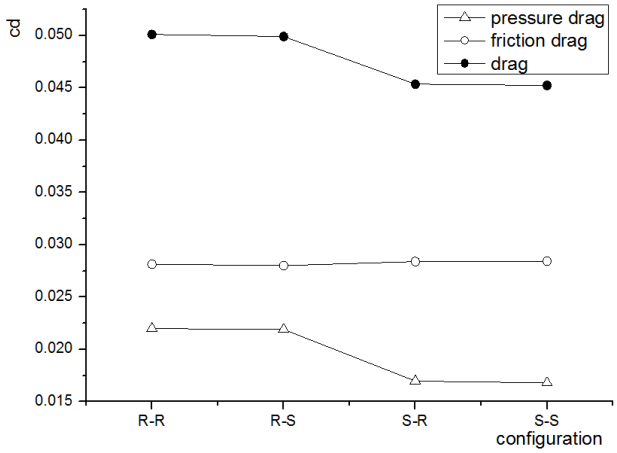

Fig. 9. Aerodynamic drag of the streamlined part of the four compositions

Table 4 Details of two heads with different slenderness

S head		R head	
γ	surface/m2	γ	surface/m2
3.3	27.5	/	/
5.0	40.1	4.8	39.7
6.6	52.8	6.4	52.3

8.3	65.7	8.0	65.1
9.9	78.5	9.6	77.8
12.4	97.9	12.0	97.0
/	/	16.0	129.1

The slenderness γ is defined by equation $\gamma = Ln / \sqrt{S / \pi}$, in which Ln is length of streamlined part and S is the cross-sectional area of the train body. Table 4 lists the details. The slenderness ratios range from 3.3 to 12.4 for S and 4.8 to 16.0 for R, and surface area of the streamlined part vary with slenderness ratio.

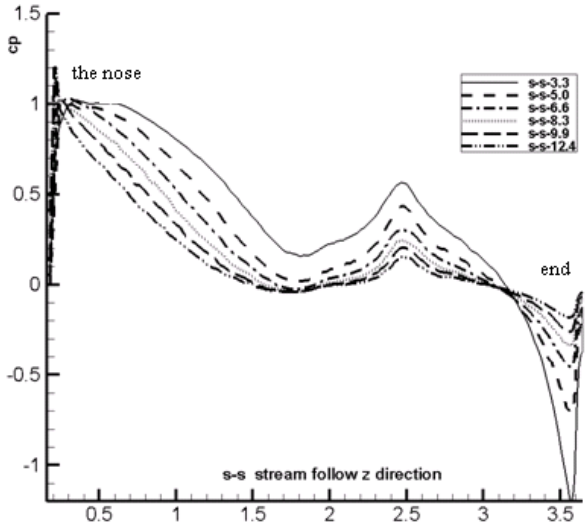

Fig. 10. Pressure coefficient along symmetrical in z-direction

It can be seen from Fig. 10, as slenderness ratio increases, the pressure coefficient decreases, especially along the nose and at the cab. At the end of streamlined part, the pressure coefficient is negative and it increases. The bigger the slenderness, the more streamlined the head will be. Because of the fluent transition of the surface curvature, the pressure on the train surface changes slowly. This is the reason why there is apparent negative pressure coefficient of the train with 3.3 and 5.0 slenderness ratios at the end of streamlined part. The train with higher slenderness ratio is of less negative pressure coefficient.

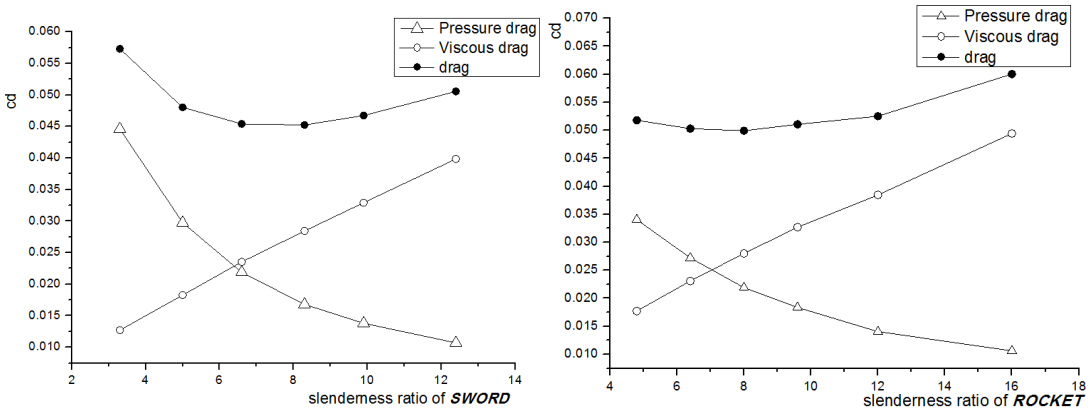

Fig. 11. Drag coefficients of S and R vary with γ changes

The curves of the pressure drag coefficient, the viscous drag coefficient, and the total drag coefficient's variation with the slenderness ratio change are shown in Fig. 11. The curves demonstrate that the viscous drag coefficient increases almost linearly, while the pressure drag coefficient decreases nonlinearly with the slenderness ratio increasing, either for the S and the R. Therefore, the total drags of both S and R meet their minimal values. Table 5 lists the detail data. We can find that the optimal slenderness ratios of S and R are 8.3 and 8.0, respectively.

Table 5 Drag coefficients of S and R vary with γ changes

γ	S head of S-S configuration Pressure drag	Friction drag	Total drag	γ	R head of R-S configuration Pressure drag	friction drag	Total drag
3.3	0.04461	0.01271	0.05732	/	/	/	/
5.0	0.02976	0.01827	0.04803	4.8	0.03405	0.01773	0.05179
6.6	0.02187	0.02353	0.04541	6.4	0.02722	0.02308	0.05030
8.3	**0.01680**	**0.02844**	**0.04524**	8.0	**0.02191**	**0.02801**	**0.04992**
9.9	0.01381	0.03293	0.04674	9.6	0.01836	0.03270	0.05106
12.4	0.01070	0.03986	0.05056	12.0	0.01406	0.03846	0.05252
/	/	/	/	16.0	0.01062	0.04943	0.06005

Fig. 12 shows the pressure drag coefficient vary with the slenderness ratio change. The figure shows that because the nose of R is blunter than S, the pressure drag of R is higher than the pressure drag of S at the same slenderness ratio point.

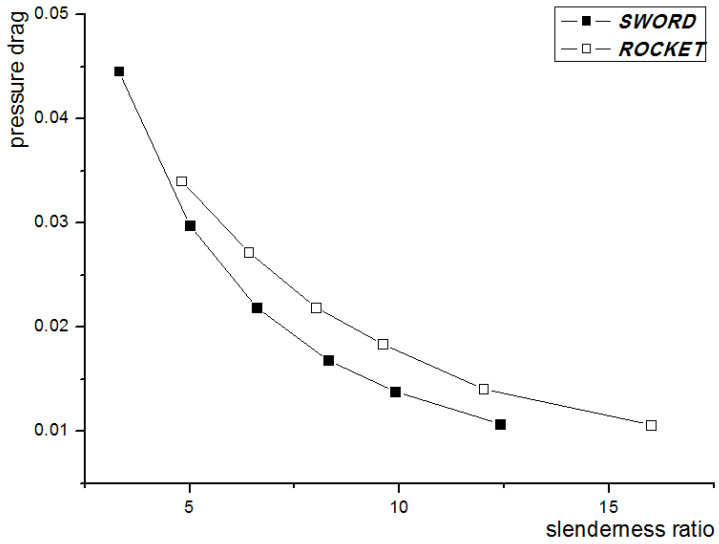

Fig. 12. Pressure drag coefficients of S and R vary with γ changes

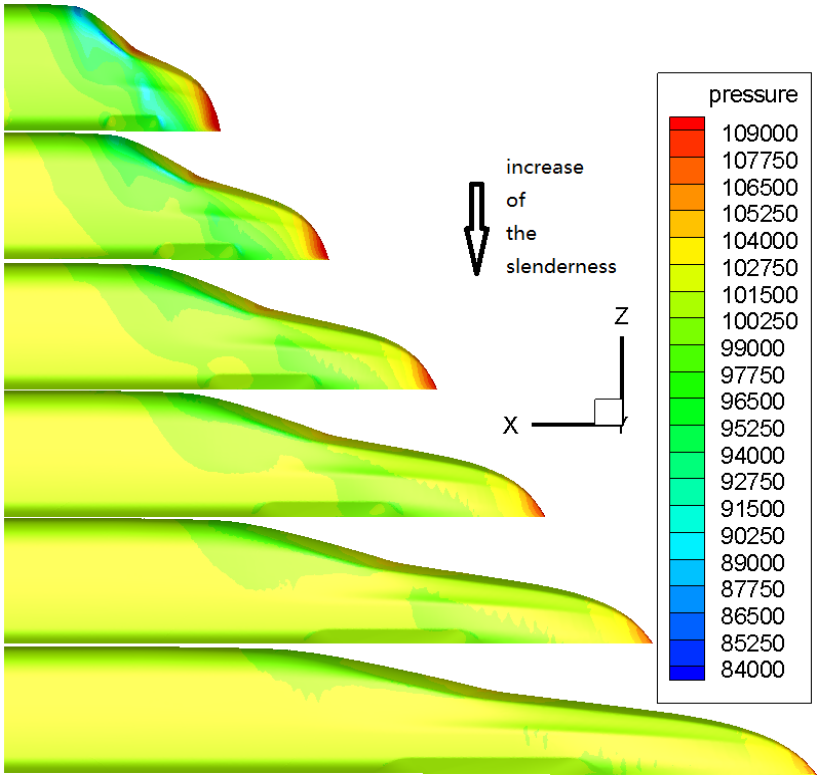

Fig. 13. Pressure contours of the streamlined part within different slenderness

Fig. 13 demonstrates the pressure contour of the streamlined part of S. It is clear that as the streamlined increased, the maximum pressure at the nose decreased gradually. When the slenderness is at 3.3, the end of the streamlined part arise the area of low pressure. The similar phenomenon can be found in the pressure contour of the streamlined part of R, shown in Fig. 14.

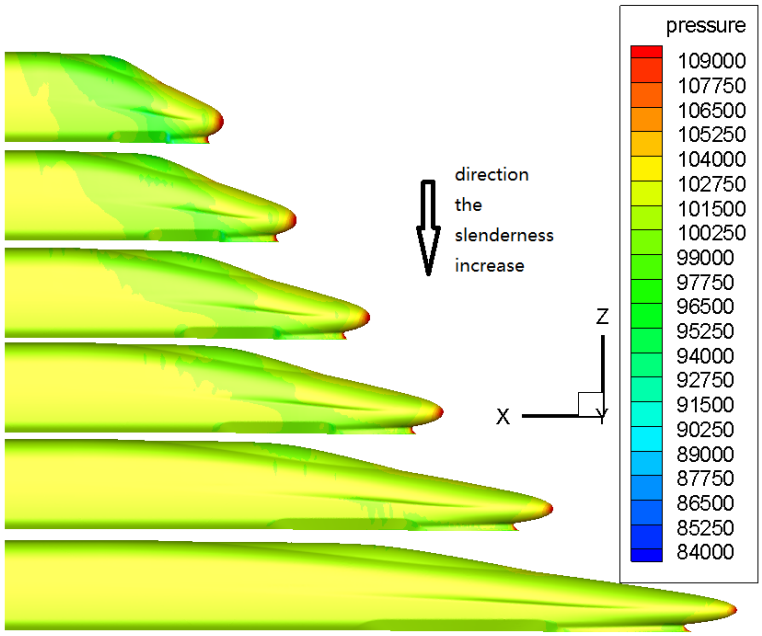

Fig. 14. Pressure contours of the streamlined part of R within different slenderness

From the above analysis, the regulations of how the head slenderness influences the aerodynamic drag of R-S and S-S are similar to each other. And the slenderness ratios are near 8.3 and 8.0 for R and S respectively, the drag coefficients come to an optimal. As the slenderness increase, the pressure drag decrease gradually and the friction increase linearly. In addition, the aerodynamic drag of the middle and tail car decrease while the head slenderness ratio increase within unsymmetrical train, while S-S has no such kind of flow-field characteristic, which means that the unsymmetrical train configuration has more room to decrease the train aerodynamic drag.

6 CONCLUSION

The study in this essay can be classified into two parts. To begin with, the aerodynamic performance of the four train configuration with three-carriage has been explored. In addition, we studied the regulation how the slenderness ratio influences the aerodynamic drag. We come to the several conclusions.

Firstly, R performances better than S as head and tail in aerodynamic drag, and R-R configuration has the largest aerodynamic drag than other three. And S-S configuration has the smallest aerodynamic drag. Considering both the aerodynamic drag and lift, the unsymmetrical train S-R is preferable as it produces the least drag and absolute value of the lift for the tail. In addition, the middle carriage of unsymmetrical train is of the less drag. The unsymmetrical train shape satisfies more than one optimal aerodynamic performance. As a result, it is efficient to design the head and tail shape respectively to obtain the optimal design of a train configuration.

Secondly, it can be concluded that the slenderness of a streamlined head impacts the aerodynamic performance in some extent. The aerodynamic drag can be classified

into two parts, the pressure drag and the friction drag. When the slenderness ratio is small, the pressure drag dominant the whole aerodynamic drag and as the head turns to be more streamlined, the friction takes up more. As the slenderness ratio becomes bigger and bigger, the pressure drag take less account but the friction turns to take more proportion. As a result, the total drag of the train drops firstly and then increases. For every train configuration, there exists an optimal slenderness ratio. For head shape R and S, the optimal slenderness ratios are about 8.3 and 8.0, respectively.

Moreover, the middle and the tail carriages tend to decreasing as the slenderness increases in the unsymmetrical train. So it can be concluded that the unsymmetrical train has much more room for optimizing the aerodynamic drag.

This essay has investigated the aerodynamic performance of unsymmetrical train and the influence caused by the slenderness ratio, with the windshields, the bogies and other components simplified. However, the above components are to impact the flow field so as to make difference to the aerodynamic performances such as lift and drag at some extent. Therefore, it is the next step to study the aerodynamic changes caused by the detail components and further validate the regulations obtained in this essay. Also, the work optimizing the head shape by numeric simulation and optimization method is to be developed for the head shape has a great impact on aerodynamic drag.

ACKNOWLEDGMENTS

The authors gratefully acknowledge the financial support provided by the Natural Science Foundation of China (National Key Project No. 90916013) and national key technology R&D program under 2009BAQG12A03.

REFERENCES

Anthoine, J., and Gouriet, J. B. and Rambaud. P. (2007) “Reduction of the sonic boom from a high-speed train entering a gallery”, AIAA-2007-3559

Baker, C. (2010). “The flow around high speed trains”, *Journal of Wind Engineering and Industrial Aerodynamics*, Vol. 98(6-7), 277-298

Chen, N. Y. and Zhang J. (1998). “experimental investigation on aerodynamic drag of high speed train”, *Journal of the China Railway Society*, Vol. 20 (5), 40-46 (in Chinese)

Chen, R. L, Zeng, Q. Y, Xiang, J., et al. (2009). “Study on the performances of aerodynamics of high-speed train with different nose shapes”. *Journal of Hunan University of Science and Technology*, Vol. 24 (1), 45-48 (in Chinese)

Lee, J. S., Kim, J. H. (2008). “Approximate optimization of high-speed train nose shape for reducing micro-pressure wave”, *Structural and Multidisciplinary Optimization*, Vol. 35, 79-87

Liang, X. F., Zhang, J. (2002). “Application of industrial visual design and aerodynamics in design of contour of streamlined train”, *Journal of Rolling Stock*. Vol. 40 (7), 05-08 (in Chinese)

Kikuchi, K., lida, M. and Fukuda. T. (2011). “Optimization of train nose shape for reducing micro-pressure wave radiation from tunnel exit”, *Journal of Low Frequency Noise, Vibration and Control*, Vol. 40 (1):890-899
Krajnovićm, S. (2009). “Optimization of aerodynamic properties of high-speed train with cfd and response surface model”, *The Aerodynamics of Heavy Vehicles II: Trucks, Business, and Trains*, Vol. 41, 197-211
Ku, Y. C., Rho, J. H., Yun, S. H. (2010). “Optimization cross-section area distribution of high-speed train nose to minimize the tunnel micro-pressure wave”, *Structural and Multidisciplinary Optimization*, Vol. 42, 965-976
Raghunathan, R. S., Kim, H. D. (2002). “Aerodynamics of high-speed railway train”, *Progress in Aerospace Sciences*, Vol. 38(6-7), 469-514
Sun, Z. X., Song, J. J. and An Y. R. (2010). “Optimization of the head shape of the CRH3 high speed train”, *Science China Technological Sciences*, Vol. 53, 3356-3364
Tian, H. Q. and Liang, X. F. (2003). “study of comprehensive aerodynamic performance for ‘china star’ high speed EMU”, *Electric Drive for Locomotives*, Vol. 13 (5): 40-45 (in Chinese)
Tian, H. Q., Zhou, D. and Xu, P. (2006). “Aerodynamic performance and streamline head shape of train”, *China Railway Science*, Vol. 27 (3), 47-55 (in Chinese)
Tian, H. Q. (2007). “Aerodynamics on high speed train”, *Beijing, China Railway Press*, 157-160 (in Chinese)
Vytla, V. V., Huang, P. G., Penmetsa, R. C. (2010). “Multi objective aerodynamic shape optimization of high speed train nose using adaptive surrogate model”, AIAA-2010-4383
Wang, X. P., Cui, K., Gao, T. Y. and Yang, G. W. (2011) “Primary study of aerodynamic performance evaluation and optimization of the high-speed train”, In: *Proceedings of the Sixth International Fluid Mechanics. Guangzhou: AIP*, 178-180